FAILURE MODES OF LAMINATE STRUCTURES

L. B. Gordon
Space Power Institute
231 Leach Center
Auburn University, Alabama 36849

R. L. Druce and M. J. Wilson
Lawrence Livermore National Laboratory
P.O. Box 808, L-153
Livermore, California 94550

Abstract

Laminate structures composed of alternating thin layers of conductor and dielectric material are commonly used in energy storage and transmission components. The failure of the dielectric layers in regions of high field stress, with applied 60 Hz ac, dc and impulse voltages, was studied. Several geometries were compared, including staggered and flush edges. Electrical trees developed between the laminated dielectric layers. The visual characteristics and growth rates of the electrical trees under ac, dc and impulse stresses were different.

Partial discharge detection and analysis was used to measure the inception voltage and discharge activity at the conductor edge voids, to observe tree formation and growth, and to predict impending failure due to dielectric erosion. Electric field distributions were modeled and partial discharge inception levels were estimated from known void geometries. The staggered edge geometry appears to enhance the electric field stress at the recessed electrode.

Introduction

Electrical insulation is a key factor to the performance attainable from pulsed power systems. The maximum energy density is limited by the breakdown strength of the dielectric and lifetime is limited the the degradation of the material upon repeated exposure to electric fields. The breakdown strength and lifetime may be further reduced by other environmental stresses such as mechanical and thermal stress. The intrinsic breakdown strength of the dielectric material is never achieved in a practical system due to the presence of defects such as voids, triple junctions, impurities, etc. These defects create regions of enhanced fields and are usually the site of failure initiation. By modeling these defects an attempt can be made to predict insulator performance.

A common insulator/conductor geometry found in many pulsed power components is the laminate structure composed of alternating layers of dielectric and conducting material. Examples of this geometry include capacitors, flat cables and high frequency magnetic cores. Dielectric failure often initiates at conductor edges due to strong field enhancement, at edge imperfections, gas-filled voids and/or at thin dielectric regions. This research is unique because it uses partial discharge detection and analysis techniques along with accurate electric field models to predict site location for failures. After a description of the models and experimental technique partial discharge measurements and degradation and failure results are given for several test samples.

Geometry and Models

The structure studied is a parallel plate stripline made with copper and Kapton layers. It is a compact, low inductance, flat cable designed to transmit high voltage pulses. This particular component was chosen for study because it is a structure common to many pulsed power components. Field calculations are relatively straightforward for this two conductor design, and the semi-transparent dielectric allows observation of the partial discharge and failure sites. The results obtained for this two conductor case are useful in understanding more complex components, for instance, capacitors where there may be multiple, alternating polarity, conducting layers; various other dielectric and conductor materials; and differing degrees of conductor width and degree of stagger.

The cable is typically composed of two 0.1 mm thick copper strips, separated and enclosed by layers of 0.05 mm thick Kapton laminate, Fig. 1.

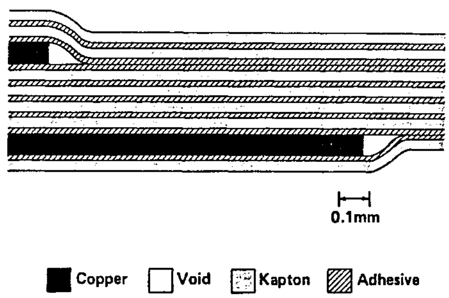

Figure 1. Cross section of cable edge showing laminations and edge voids.

The Kapton layer between the two copper strips is composed of three or four layers of 0.05 mm thick Kapton film, and the upper and lower Kapton layers covering the copper strips are composed of one to two layers of Kapton. The copper and Kapton layers are bonded together with an adhesive, an individual layer of which is approximately 0.02 mm thick. The example shown in Fig. 1 (not to scale) has four layers of Kapton between the two copper electrodes, two above and one below. The cross sectional view shows only the edge region and

* Work performed under the auspices of the U.S. Department of Energy by the Lawrence Livermore National Laboratory under contract number W-7405-ENG-48.

Report Documentation Page

Form Approved
OMB No. 0704-0188

1. REPORT DATE **JUN 1987**	2. REPORT TYPE **N/A**	3. DATES COVERED **-**
4. TITLE AND SUBTITLE **Failure Modes Of Laminate Structures**		5a. CONTRACT NUMBER
		5b. GRANT NUMBER
		5c. PROGRAM ELEMENT NUMBER
6. AUTHOR(S)		5d. PROJECT NUMBER
		5e. TASK NUMBER
		5f. WORK UNIT NUMBER
7. PERFORMING ORGANIZATION NAME(S) AND ADDRESS(ES) **Space Power Institute 231 Leach Center Auburn University, Alabama 36849**		8. PERFORMING ORGANIZATION REPORT NUMBER
9. SPONSORING/MONITORING AGENCY NAME(S) AND ADDRESS(ES)		10. SPONSOR/MONITOR'S ACRONYM(S)
		11. SPONSOR/MONITOR'S REPORT NUMBER(S)

12. DISTRIBUTION/AVAILABILITY STATEMENT
Approved for public release, distribution unlimited

13. SUPPLEMENTARY NOTES
See also ADM002371. 2013 IEEE Pulsed Power Conference, Digest of Technical Papers 1976-2013, and Abstracts of the 2013 IEEE International Conference on Plasma Science. Held in San Francisco, CA on 16-21 June 2013. U.S. Government or Federal Purpose Rights License

14. ABSTRACT
Laminate structures composed of alternating thin layers of conductor and dielectric material are commonly used in energy storage and transmission components. The failure of the dielectric layers in regions of high field stress, with applied 60 Hz ac, de and impulse voltages, was studied. Several geometries were compared, including staggered and fiush edges. Electrical trees developed between the laminated dielectric layers. The visual characteristics and growth rates of the electrical trees under ac, de and impulse stresses were different.

15. SUBJECT TERMS

16. SECURITY CLASSIFICATION OF:			17. LIMITATION OF ABSTRACT	18. NUMBER OF PAGES	19a. NAME OF RESPONSIBLE PERSON
a. REPORT **unclassified**	b. ABSTRACT **unclassified**	c. THIS PAGE **unclassified**	**SAR**	**5**	

Standard Form 298 (Rev. 8-98)
Prescribed by ANSI Std Z39-18

illustrates the gas voids at the edge of the conductors trapped by the laminating process, and the conductor stagger, where the copper edges do not line up but are staggered.

The cables studied are typically 3 to 4 cm wide, or more than 100 times the separation distance between the copper layers resulting a large region of "quasi" uniform electric field in the center of the cable. The majority of the dielectric degradation and failure took place at the cable edges where the electric field is highly nonuniform. Two cases of electrode stagger were studied: flush where the upper and lower copper foils edge simultaneously, and staggered where the stagger is 2 mm or approximately 10 times the separation distance. The copper layers have cut edges and the Kapton layers merge to join, such that there is a significant void at the edge of each copper layer. The exact dimensions and content of the voids are unknown, but visual observation tends to indicate that the voids most likely contain air at atmospheric pressure, and have cross sectional dimensions of about the thickness of the copper, 0.1 mm.

For the electric field distribution models the relative permittivity of the adhesive was assumed to be the same as the Kapton ($\varepsilon_r = 3.5$) and the void was assumed to be air ($\varepsilon_r = 1$). Thus, the multiple layered construction shown in Fig. 1 reduces to the simpler case in Fig. 2. Outside the cable was air ($\varepsilon_r = 1$) or fluorinert ($\varepsilon_r = 1.86$) a dielectric fluid used to suppress external partial discharges.

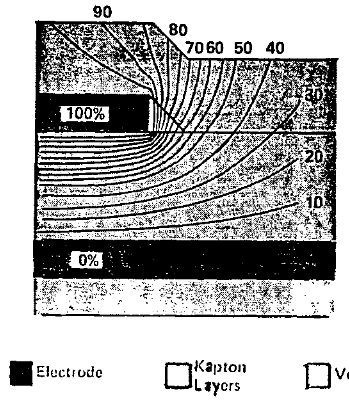

Figure 2. Equipotential contour lines for staggered edge geometry electrodes.

Electric field calculations were performed for the edge regions varying three parameters: (1) the presence of edge voids (void or no void), (2) the presence of edge stagger (flush or staggered), and (3) the external dielectric medium (air or fluorinert). Figure 3 illustrates the contours of potential, or equipotential lines, for a flush edge geometry cable with no air voids immersed in air. Figure 4 illustrates the contours of constant electric field (expanded view) of a conductor edge with a void.

The results from the electric field stress models are summarized in Fig. 5. The electric field strength is normalized to the value of the field in the quasi-uniform region between the two conductors far from the edge. For instance, in Fig. 5a, the normalized electric field strength for two flush edges without voids has a value of 1 at the outside corners and a value of 2 at the inside corners. Thus, the magnitude of the electric field strength at the outside corners is equal to that found in the uniform field region, while the magnitude of the electric field strength at the inside corners is twice that in the uniform field region.

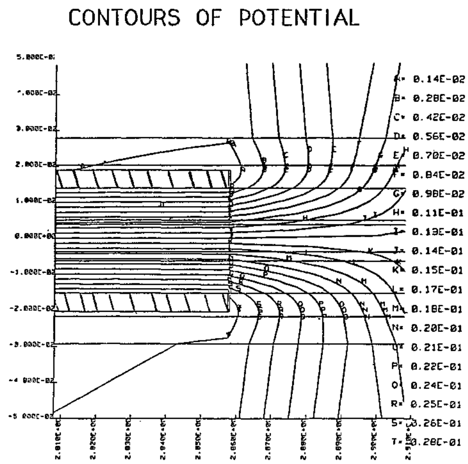

Figure 3. Equipotential contour lines for flush edge geometry electrodes.

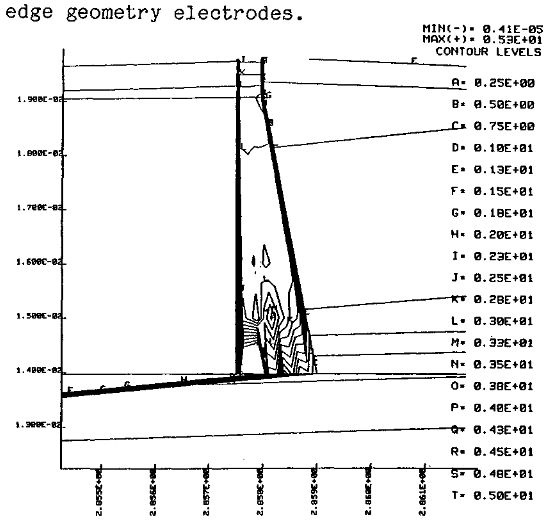

Figure 4. Equipotential contour lines at an electrode edge with a void.

The following conclusions were reached from the electric field stress models:

- o The nonuniformity of the electric field at the edge of a parallel plane geometry results in an increased stress of X2 at the inside corners.
- o Whereas the direction of the electric field in the uniform region is totally in the Y direction (orthogonal to the conductors) the enhanced field (for all cases) at the edges was due to a significant X component (parallel to the conductor/dielectric layer boundaries).
- o The effect of voids at the edge of the conductors was to increase the electric field stress by approximately 50 percent both at the inner and outer corners, Fig. 5a.
- o By staggering the two conductor edges, the electric field stress was reduced at the retracted edge (note the reversal in the relative magnitude of the inner and outer

values), but the stress was increased at the inner corner of the extended edge, Fig. 5b.

- If fluorinert were used as the surrounding dielectric for the cable instead of air additional flux was "forced" into the void region resulting in increased electric field stress at the edges, Fig. 5c.

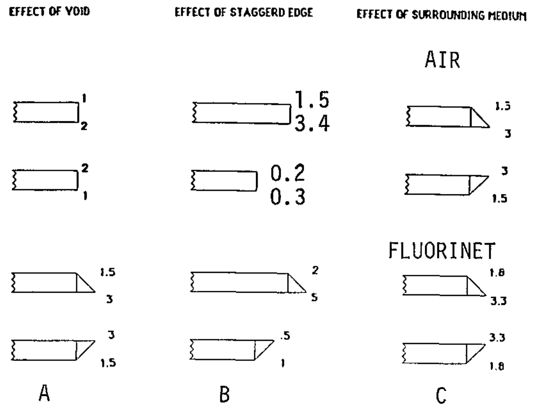

Figure 5. Normalized electric field strength for different electrode geometries.

Results of the electric field stress models indicate that the highest field stress will occur at conductor edges, presence of edge voids will significantly enhance field stress, and the staggered edge geometry will increase stress at the extended electrode. In addition, the breakdown strength of the gas in the void should be considerably less than that of the solid dielectric indicating a strong possibility for partial discharges in the void region. The partial discharges will occur along the field lines with a component in the X direction. The adhesive layer (lying in the X direction) will have a lower breakdown strength and most likely less chemical resistance to decay by partial discharge.

Experimental Technique

Partial discharges are measured under a 60 Hz ac applied voltage and are recorded with a multichannel pulse height analyzer. Figure 6 shows the main components of the discharge detection system, which includes a voltage source and pulse coupling through a detection circuit. The ac power supply is a low-noise design to reduce interference with the partial discharges from the power source.

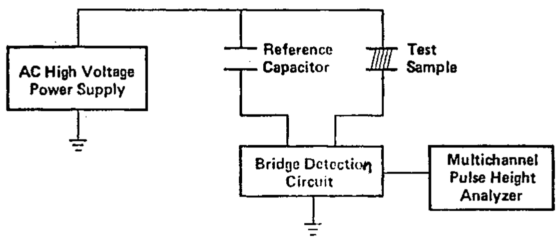

Figure 6. Ac partial discharge test circuit.

The detection circuit used is a balanced bridge feeding a pulse shaping preamp. The signal is then captured by a multichannel pulse analyzer system where it is amplified, digitized, and recorded under computer control. The accumulated data is displayed as a signature of the number of pulses versus the size of the pulse (in pC). An example signature is shown in Fig. 7. For these cable studies, the analyzer system was usually set to record pulses to 8000 pC, with a pulse resolution of 2 pC. A few measurements near end-of-life were made with 80 nC full scale and 20 pC resolution. The system was calibrated by injection of a 10 pC pulse into the detection loop.

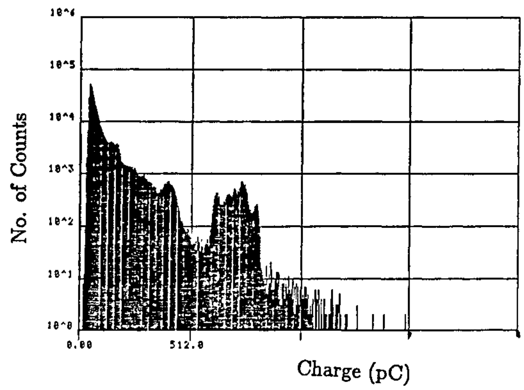

Figure 7. A charge spectrum shows the distribution of individual discharges as a function of charge quantity.

In this study, the interest was in prediction of failure sites, failure modes, and detection of the aging process. Since the cable is intended for pulse operation, the aging was introduced by pulsed voltages. The pulses were 15 kV with a decay of 5 µs, produced by discharging a 6 nF capacitor through a 200 ohm load. The pulses were applied at a repetition rate of 50 impulses per minute.

Partial discharge signatures were measured after 50, 250, 500, and thereafter every 500 shots. In addition, visual examination for occurrence and growth of electrical tree channels at the conductor edges were made at these intervals. The ac voltage test levels were selected to be just above the inception level and at moderate overvoltages. For the cable studied here, these test voltages were 2, 3, and 4 kV rms. The 4 kV level was determined to be nondestructive compared to the pulse aging studies, since test measurements revealed no change in partial discharge signature before and after 12 hours of ac operation at 4 kV, and ac cable life was more than 6 hours at three times the test voltage (12 kV rms).

In addition to the pulsed failure tests, a few cable specimens were stressed under high ac (15 kV rms) and high dc (15 kV) to observe degradation differences.

Results

Partial Discharge Signatures

Partial discharge (PD) signatures obtained with the ac monitoring voltage showed significant changes after cables had been aged by repeated impulse voltages. Initial tests after just 50

impulses showed no PD signature change. However, by 250 impulses, a noticeable increase in PDs above 1500 pC had occurred, and by 500 impulses, PDs were regularly exceeding 4000 pC. The PD inception voltage for the cables was typically about 1.5 kV rms. This value is consistent with gas breakdown in a void of these dimensions at a conductor edge.

Cables exposed to large numbers of shots exhibited continued change in their PD signatures. In particular, larger and larger PD events would be registered. For example, after 6000 impulses PDs extending to 80,000 pC occurred. These were measured just prior to cable failure and are shown in Fig. 8.

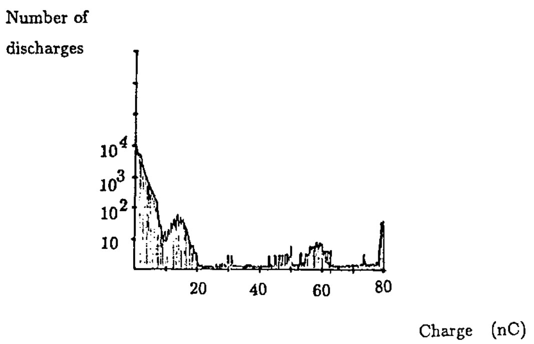

Figure 8. Partial discharge signature changes drastically just prior to cable failure.

Electrical Treeing

Coincident with major changes in the partial discharge signature there were morphology changes in the dielectric. Electrical trees were observed originating at the conductor edges and propagating in the adhesive region between the Kapton layers. This tree growth was noticeable after 500 impulses. Figure 9 shows a typical tree for the 500 impulse case through an optical microscope. Tens of these trees where observed along the cable edge and they were typically 1 to 2 mm long.

When under impulse aging tests, dark room observations of the edge region showed visual light emissions from the tree regions. As the cable was exposed to more and more impulses, the light emission became brighter and was spread over more of the length of the edge region, indicating growth of the electrical trees.

Cable Failure

After continued aging (under ac, dc, or impulse) cable failure occurred. Under impulse, aging failure occurred after approximately 7000 shots and the mode was by puncture from an extended tree through the central Kapton layer to the upper electrode region. These failures occurred shortly after the appearance of the very large (80,000 pC) partial discharges in the ac monitoring tests.

The supply of cables was limited so that testing a large number of cables for degradation and failure modes was not possible. However, from the 15 to 20 cables that failed, the following observations resulted.

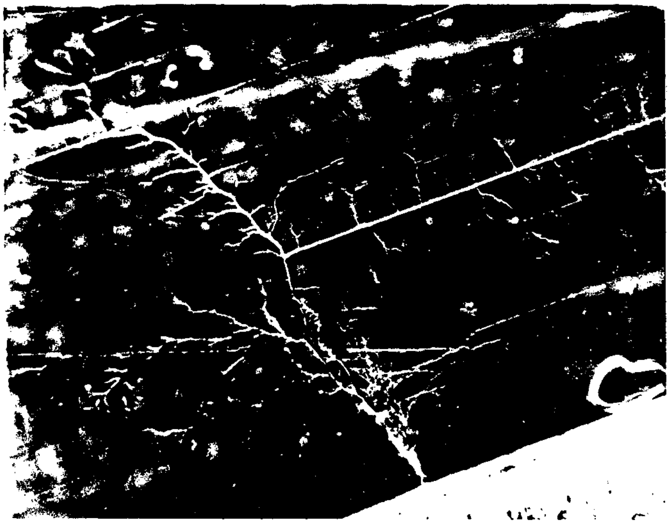

Figure 9. Impulse tree formation after 500 applied pulses.

o Tree development showed differing characteristics under ac, dc, and impulse stresses. Dc and impulse trees (Figure 10) were very similar, but ac (Figure 11) electrical trees were darker and had a larger degree of branching.

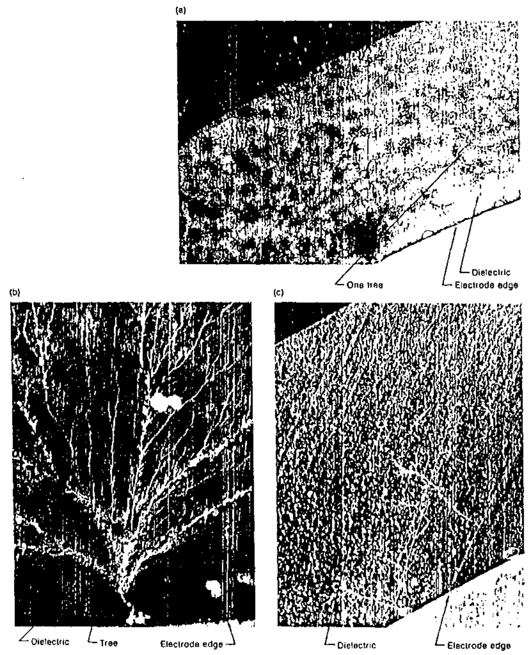

Figure 10. Comparison of dielectric degradation caused by three types of high-voltage stresses. We observed that, for two-conductor flat cable, trees form in the dielectric separating the conductors when (a) ac, (b) dc, and (c) impulsive high voltages are applied.

o Failure rarely occurred in the uniform field region (1 out of 20) and was most likely due to a dielectric defect (thin Kapton region) or assembly defect (included field emission point). All other failures occurred at edges.

- Failure with and without voids could not be compared since all cables had voids.
- Failure was always preceded by electrical tree development along the adhesive interface region.

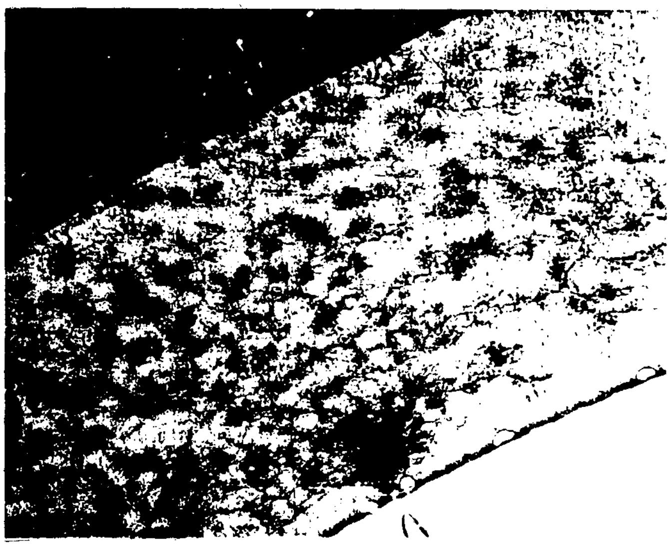

Figure 11. Ac tree formation showing a larger degree of branching.

- Under ac failure staggered edges did have a shorter lifetime than flush edges.

Conclusions

Partial discharge analysis techniques with ac steady-state voltages were successfully used to nondestructively observe the degradation and predict the failure of high voltage pulsed power insulation structures. Electric field stress models predicted sites of highest field enhancement and predicted partial discharge and failure locations.

Analysis and tests on a stripline structure demonstrated that: (1) conductor edges are regions of high field stress, (2) gas voids at conductor edges are especially detrimental, (3) staggered edge geometries may not necessarily be optimum, and (4) the adhesive layer is a weak dielectric region prone to degradation and partial discharges.